

Application of principal component analysis and wavelet transform to fatigue crack detection in waveguides

Marcello Cammarata¹, Piervincenzo Rizzo^{2*}, Debaditya Dutta³, and Hoon Sohn⁴

¹Laboratory for NDE and Structural Health Monitoring studies, Department of Civil and Environmental Engineering, University of Pittsburgh, 963 Benedum Hall, 3700 O'Hara Street, Pittsburgh, PA 15261, USA

²Department of Civil and Environmental Engineering, University of Pittsburgh, 949 Benedum Hall, 3700 O'Hara Street, Pittsburgh, PA 15261, USA

³Department of Civil and Environmental Engineering, Carnegie Mellon University, 5000 Forbes Avenue, Pittsburgh, PA 15213, USA

⁴Department of Civil and Environmental Engineering, Korea Advanced Institute of Science and Technology, Daejeon 305-701, Korea

(Received December 15, 2008, Accepted July 29, 2009)

Abstract. Ultrasonic Guided Waves (UGWs) are a useful tool in structural health monitoring (SHM) applications that can benefit from built-in transduction, moderately large inspection ranges and high sensitivity to small flaws. This paper describes a SHM method based on UGWs, discrete wavelet transform (DWT), and principal component analysis (PCA) able to detect and quantify the onset and propagation of fatigue cracks in structural waveguides. The method combines the advantages of guided wave signals processed through the DWT with the outcomes of selecting defect-sensitive features to perform a multivariate diagnosis of damage. This diagnosis is based on the PCA. The framework presented in this paper is applied to the detection of fatigue cracks in a steel beam. The probing hardware consists of a PXI platform that controls the generation and measurement of the ultrasonic signals by means of piezoelectric transducers made of Lead Zirconate Titanate. Although the approach is demonstrated in a beam test, it is argued that the proposed method is general and applicable to any structure that can sustain the propagation of UGWs.

Keywords: ultrasonic guided waves; principal component analysis; fatigue crack detection; structural health monitoring.

1. Introduction

Steel structures are ubiquitous in mechanical, industrial and civil engineering systems. Failure of these structures is often attributed to fatigue or fracture cracks. As in most cases cracks cannot be avoided, there is a need for non-destructive inspection (NDI) or structural health monitoring (SHM) techniques aimed at detecting structural deficiencies at early stage of deterioration.

NDI techniques such as acoustic emission (Roberts and Talebzadeh 2003), eddy current (Sophian *et al.* 2001), ambient-vibration based (Chondros *et al.* 1998), and impedance-based methods (Giurgiutiu and Rogers 1997, Park *et al.* 2003) were proposed for the detection of cracks in steel structures. Methods based on ultrasonic guided waves (UGWs) gained increasing popularity owing to the

*Corresponding Author, Assistant Professor, E-mail: pir3@pitt.edu

capability of inspecting moderately large areas using a single probe attached or embedded in the structure while maintaining high sensitivity to small flaws (Alleyne and Cawley 1996, Rose 1999, Staszewski 2003, Kundu 2004, Giurgiutiu 2005, Rizzo and Lanza di Scalea 2007). UGWs and particularly Lamb waves were successfully used to monitor the propagation of fatigue cracks in plate-like metallic structures (Worden *et al.* 2000, Fromme and Sayir 2002, Fromme *et al.* 2004, Leong *et al.* 2005, Park *et al.* 2006, Staszewski *et al.* 2007, Kim and Sohn 2008, Dutta *et al.* 2008).

In the last decade the need for signal processing and pattern recognition in the fields of guided waves became evident to enhance the capability to detect size, locate and classify damage.

This paper presents a monitoring scheme based on discrete wavelet transform (DWT) and principal component analysis (PCA). Particularly, this study focuses on the onset and growth of fatigue cracks, which is relevant to predict the remaining life of steel structure. The DWT is known to be effective to de-noise and compress signals and to extract features that are sensitive to the presence of damage (Mallat 1989, 1999, Paget *et al.* 2003, Rizzo and Lanza di Scalea 2005, 2006, 2007, Rizzo *et al.* 2007). The PCA is a statistical technique introduced in 1901 (Pearson 1901) and developed independently thirty years later (Hotelling 1933) adopted in several fields spanning from medicine, to finance and engineering to reduce the dimensionality of data (Flury 1988, Duntelman 1989, Jolliffe 2002). In SHM applications PCA was used for data compression, pattern recognition, and damage interpretation (Manson *et al.* 2001, Johnson 2002, Sohn *et al.* 2002, Rippengill *et al.* 2003, Mustapha *et al.* 2005, 2007, Ni *et al.* 2006, Yan *et al.* 2005a, 2005b, Tong *et al.* 2006).

The present study complements an ongoing effort aimed at identifying fatigue cracks in structural waveguides (Rizzo *et al.* 2009, Dutta *et al.* 2009). The scheme presented here uses a set of features extracted from unprocessed ultrasonic signals and from signals processed with the DWT. These features represent the element of a multi-dimensional damage index vector which is fed to a PCA. It is demonstrated that the PCA increases the sensitivity to detect damage and that the selection of the input vector is essential to improve the performance of the algorithm.

The algorithm presented here is applied to the detection of fatigue cracks in a steel beam. The probing hardware consists of wafer piezoelectric transducers (PZTs) used for both ultrasound generation and sensing. These PZTs are suitable for SHM applications as they are easy to attach to the structure surface or to embed in the structure.

2. Experimental setup

The experiment was performed on a 2.74 m long W6 × 15 (SI: W150 × 22.5) steel beam conforming with ASTM A36 material specifications. The dimensions of the steel section are shown in Fig. 1. Two notches were cut into the bottom (tension) flange near the center of the beam-span as shown in Fig. 1(b). These notches served as fatigue crack initiators, and also helped to increase the stress at this section in order to accelerate the development of fatigue cracks. The notches were designed to have a theoretical fatigue life on the order of 40,000 cycles at an applied stress range of 190 MPa. Notches on either side of the web were the same to mitigate any eccentric behavior. Fatigue cracks were expected to form at the sharp root of each notch. Four electrical resistance crack propagation gages were employed to monitor the onset and growth of the fatigue cracks. These gages were attached at both notch roots on the upper and lower surfaces of the flange (Fig. 2).

The test bed was designed to be simply a vehicle to fatigue crack initiation and growth. Thus, specimen having a predictable fatigue behavior, at a reasonable scale, and in a reasonably short time

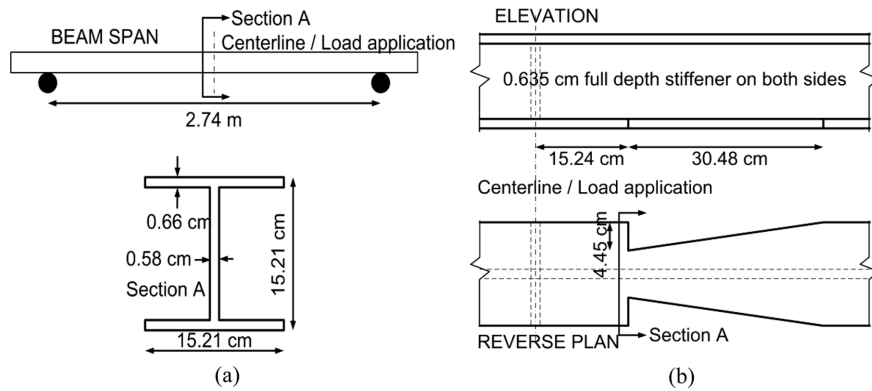


Fig. 1 Dimensions of the steel $W6 \times 15$ (SI: $W150 \times 22.5$) section, (a) beam span and cross section and (b) elevation and plan views of the flange in the tension side

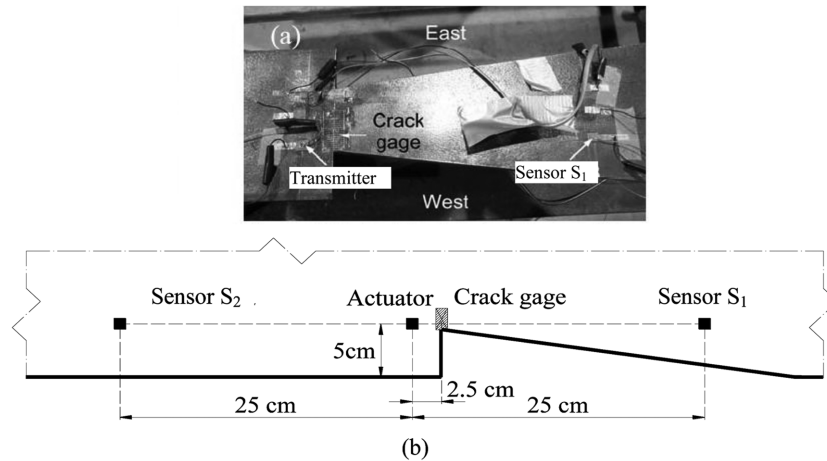


Fig. 2 (a) Photo of the part of the tension flange of the steel beam with PZT emitter and PZT sensor S_1 receiver (PZT-B) and (b) schematic figure showing the transmitter and both sensors

period is required.

To produce the cracks, the beam was loaded in simple mid-span loading over a span length of 2.74 m. The midspan load was cycled from 4.5 kN to 40.5 kN resulting in a load range of 36 kN. Cycling was carried out using a sinusoidal function at 1 Hz rate. The 36 kN applied load corresponds to a tensile stress range of 190 MPa at the notch root of the tension flange. The minimum stress, at an applied load of 4.5 kN is 22.7 MPa. The notch site was continuously monitored for crack initiation.

Fig. 3(a) shows the history of crack propagation in both west and east flanges of the steel beam as a function of the number of loading cycles. After approximately 9,000 cycles, cracks at each notch root were identified by the crack gages and could be observed visually. As the resolution of the crack gages was 0.25 mm, any crack smaller than this value could not be captured. Following every few thousand cycles, the cyclic loading was paused and a static load of 22 kN (average of fatigue load stress range) was applied to the beam.

Three PSI-5A4E type PZT wafer transducers ($1.0 \text{ cm} \times 1.0 \text{ cm} \times 0.051 \text{ cm}$) were mounted on the bottom flange of the beam. One transducer acted as a transmitter and was placed in between the

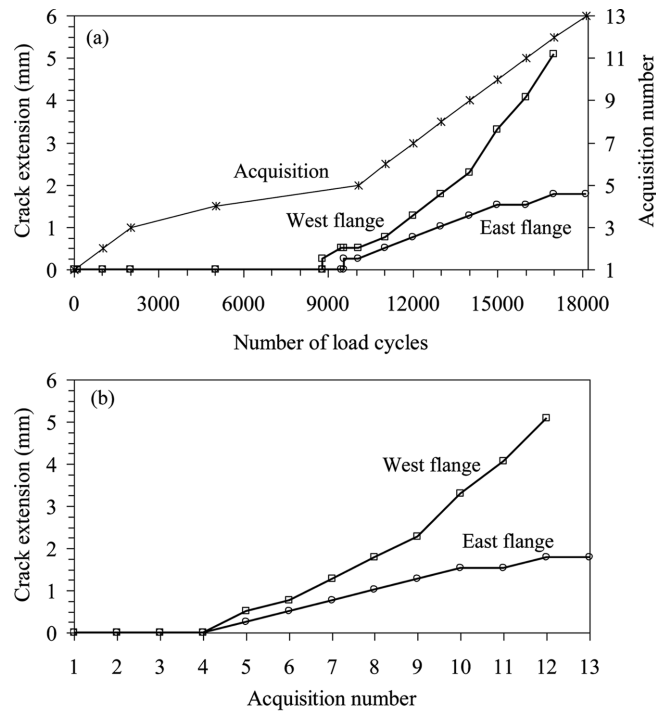


Fig. 3 (a) Propagation history of the crack emanating from the notch-tip of west and east part of the tension flange of the steel beam as a function of the number of loading cycles. The acquisition (ultrasonic measurement) number history is superimposed and (b) crack extension recorded by both crack gages as a function of the acquisition (ultrasonic measurement) number

two sensors S_1 and S_2 which were located 50 cm apart (Fig. 2). The crack initiator fell between the transmitter and sensor S_1 . A National Instruments PXI[®] unit running under LabVIEW[®] was employed for signal excitation, detection and acquisition. Five-cycle 10 volts peak-to-peak (ppk) 225 kHz toneburst modulated with a Hann window were used as excitation signals. The signals were sampled at 10 MHz and averaged ten times prior to storage to increase the signal-to-noise ratio.

Under the static load of 22 kN the data from the two PZT sensors were collected. A total of thirteen acquisitions were made. The acquisition numbers as a function of the number of load cycles is superimposed in Fig. 3(a). The relationship between the acquisition number and the extension of damage as recorded by the crack gages is shown in Fig. 3(b).

The selection of the driving frequency of 225 kHz was chosen for this analysis based upon the outcomes of a simultaneous study (Rizzo *et al.* 2009). Based on the Rayleigh-Lamb wave equation in plate structures (Rose 1999), only the first symmetric S_0 and the first anti-symmetric A_0 modes can propagate along the bottom flange of the specimen under investigation.

Typical waveforms detected at the beginning and at the end of the fatigue loading protocol are shown in Fig. 4. Fig. 4(a) shows the time history recorded by sensor S_1 when the structure was pristine. Owing to the different group velocities, the S_0 mode is clearly separated from the A_0 mode. Some ultrasonic trace is visible after the A_0 mode. This is the effect of mode scattering when the waves pass through the notch and of reflections with the boundaries. The time waveform recorded by sensor S_2 and shown in Fig. 4(b) suggest that the A_0 mode may interfere with the symmetric

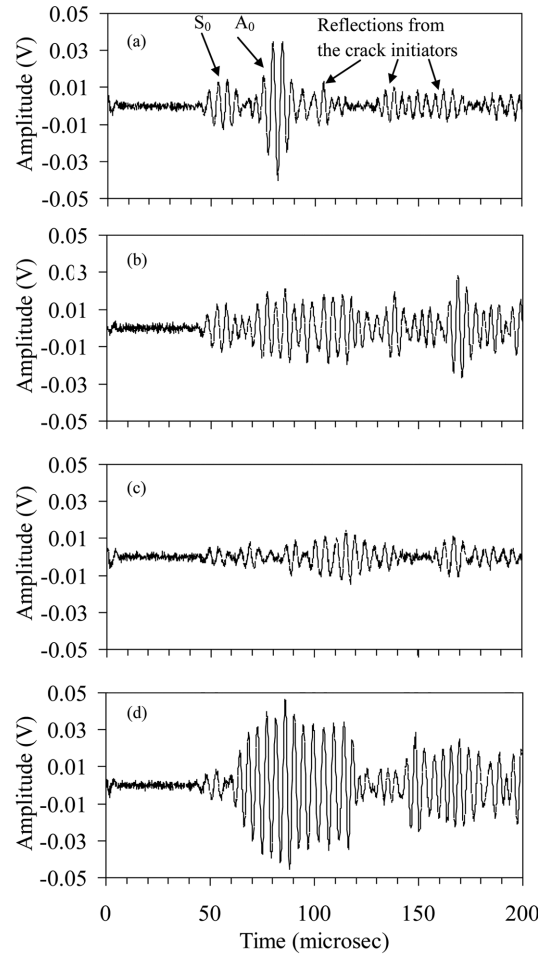


Fig. 4 Typical waveforms recorded by (a) sensors S_1 at cycle 0, (b) sensors S_2 at cycle 0, (c) sensors S_1 at cycle 18,000 and (d) sensors S_2 at cycle 18,000

mode traveling toward sensor S_1 and partially reflected from the crack initiators notches. This justifies the higher acoustic energy detected by sensor S_2 at the completion of the fatigue loading protocol (Fig. 4(d)) with respect to pristine conditions (Fig. 4(b)). The decrease of the acoustic energy detected by sensor S_1 after 18,000 cycles is visible in Fig. 4(c) and it is the straightforward consequence of the presence of the fatigue cracks along the path between the transmitter and the receiver.

3. Structural health monitoring algorithm

The first step of the SHM algorithm implemented in this paper consisted of increasing the statistical population of the data. The noise was created by the MATLAB *randn* function that generates arrays of random numbers whose elements are normally distributed with zero mean and standard deviation equal to 1. The function was pre-multiplied by a factor that determines the noise level. A factor equal to 0.001 was considered to obtain a noise function representative background

noise of the stored waveforms. For this purpose white Gaussian noise was added to the ultrasonic signals. For each acquisition 19 noise-corrupted signals were obtained. Thus, a total of 20×13 (the latter represents the number of acquisitions over the entire fatigue loading protocol) = 260 time histories were available. It should be pointed out that to increase the statistical population other solutions can be used by simply increasing the number of acquisitions, or, as suggested by Gupta *et al.* (2007) by triggering the sensing hardware to the peak of the sinusoidal fatigue cycle.

Each waveform was windowed in order to divide the S_0 mode from the A_0 mode and to separate the latter mode from the spurious signals at the tail. By operating such a time windowing any effect due to mode conversion, scattering from the crack initiators notches, and reflections from the boundaries was ignored.

Ultrasonic signals were processed through the DWT, which decomposes the original time-domain signal by computing its correlation with a short-duration wave called the mother wavelet that is flexible in time and in frequency (Mallat 1989, 1999, Paget *et al.* 2003). DWT processing consists of two main parts: decomposition and reconstruction. The decomposition phase transforms the ultrasonic signal into wavelet coefficients following hierarchical levels of different time and frequency resolution. Each level contains the signal information both in the time and the frequency domain over a certain frequency bandwidth. The filtering outputs are then downsampled. De-noising of the original signal can be achieved if only a few wavelet coefficients, representative of the signal, from one or more levels are retained and the remaining coefficients, related to noise, are discarded. In the reconstruction process, the coefficients are upsampled to regain their original number of points and then passed through reconstruction filters. The reconstruction filters are closely related but not equal to those of the decomposition.

In the present study, the Daubechies mother wavelet of order 40 (db40) was considered. In previous publications (Rizzo and Lanza di Scalea 2005, 2006, 2007), it was demonstrated that the db40 is suitable for the de-noising, compression and feature extraction of narrowband signals propagating in waveguides such as strands and rails.

In the present study, the eight largest wavelet coefficient moduli from the decomposition level associated with the frequency of the generated tonebursts were chosen. Eight coefficients were considered a good tradeoff between computational agility and significative representation of the driving signal.

In this study, six statistical features, namely the variance (var), the root mean square (RMS), the maximum amplitude (max), the peak-to-peak (ppk), the K factor, and the crest factor (CF) were considered. Given a discrete signal x made of N points and average \bar{x} , such features are defined as

$$\begin{aligned} \text{var} &= \frac{1}{N} \sum_{i=1}^n x_i - \bar{x} & RMS &= \sqrt{\frac{1}{N} \sum_{i=1}^N x_i^2} & ppk &= \max(x_i) - \min(x_i) \\ Kfactor &= \max(x_i) * RMS & CF &= \max(x_i) / RMS \quad (i = 1, \dots, N) \end{aligned} \quad (1)$$

In the framework of the present UGWs based SHM approach, the function x was the unprocessed ultrasonic signal, the wavelet coefficient vector, or the reconstructed (de-noised) ultrasonic signal.

The features were used to compute a damage index defined as the ratio between a given feature F_{S_2} calculated from the signal detected by sensor S_2 , over the same feature F_{S_1} extracted from sensor S_1

$$D.I. = \frac{F_{S_2}}{F_{S_1}} \quad (2)$$

The inverse of Eq. (2) was calculated as well and the algorithm selects the highest scalar between the two. The selected scalar was then assembled to form a multi-dimensional index vector fed into the PCA algorithm.

PCA is a mathematical algorithm used to reduce the dimensionality of a data set for compression, pattern recognition and data interpretation. The algorithm projects, by a linear transformation, a high p -dimensional data vector \mathbf{X} into a new lower q -dimensional data vector \mathbf{Z} , known as principal components (Rippengill *et al.* 2003). Given N data $X_i = (x_{1i}, x_{2i}, \dots, x_{pi})$ where $i = 1, \dots, N$, the reduced data vector is $Z_i = (z_{1i}, z_{2i}, \dots, z_{qi})$, whose elements are the linear combination of the original x_{ji} ($j = 1, \dots, p$) elements. Specifically z_{1i} is the linear combination having maximal variance; z_{2i} is the linear combination which explains most of the remaining variance and so on. If the p -coordinates are a linear combination of $q < p$ variables, the first q principal components will completely characterize the data and the variance in the observed data corresponding to the remaining $p - q$ coordinates would be zero. For the analytical formulation, the interested reader may refer to (Sharma 1996, Manson *et al.* 2001, Mustapha *et al.* 2005, Tong *et al.* 2006, Yan *et al.* 2005a, 2005b) the PCA algorithm was implemented using Singular Value Decomposition as in (Sharma 1996, Mustapha *et al.* 2005, 2007).

4. Experimental results

4.1 Damage index analysis

In this section, the results from the single feature-based damage index are presented. Particularly, the results from the RMS-based damage index of the original signal, the wavelet coefficient vector and the reconstructed signal are discussed.

Fig. 5 shows the value of the RMS-based damage index as a function of the sample number. The values associated with samples 1 through 60 may be considered as baseline data. The data beyond sample number 80 are associated to the data acquired after 10,000 cycles when the crack gages determined the onset and propagation of damage (Fig. 3(a)).

The results related to the propagation of the A_0 and the S_0 modes are presented in Figs. 5(a) and 5(b), respectively. Steps are visible in both plots every 20 sample numbers. Such steps reflects the circumstance that between two consecutive acquisition the size of the crack increased. The values associated with baseline data are close to 1 when related to the propagation of the symmetric mode (Fig. 5(b)) and show a slight stepwise response when related to the propagation of the A_0 mode (Fig. 5(a)). It is argued that this behavior is due to the interference of the reflections at the signal's tail.

By observing Fig. 5(a), the RMS-based damage index computed from the vector of the wavelet coefficients is more sensitive to detect the increase of the flaw size than the other two. This suggests that accurate mode selection and signal processing may improve the sensitivity to the presence of damage. The damage index related to the propagation of the symmetric mode denotes a rapid increase from baseline and damaged conditions. For this mode, processed data slightly outperform the unprocessed (original time waveforms) data.

Finally, it worth noting that the sample interval 61-80, associated with acquisition 4, was left undetermined. Fig. 3(b) indicates that at this acquisition the beam was intact. However, both Figs. 5(a) and 5(b) show a slight step of the damage-index value.

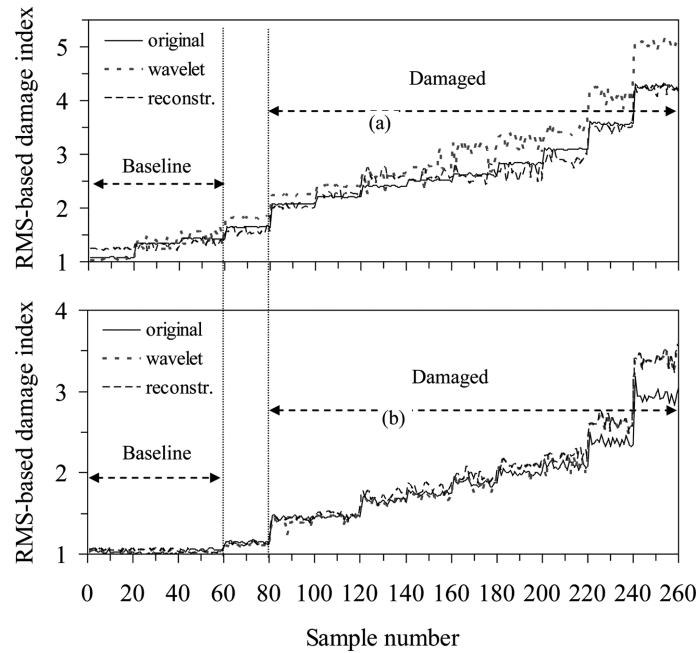


Fig. 5 RMS-based damage index as a function of the sample number, (a) analysis of the propagation of mode A_0 and (b) analysis of the propagation of mode S_0

4.2 PCA analysis

The PCA was performed on the $[6 \times 260]$ matrix containing the six statistical features selected in this study and calculated for the 260 samples. After performing the PCA, the first two component scores were retained and plotted against each other. The approach will allow the visualization of the various damage conditions by transforming the 6-dimensional damage index space into a 2-dimensional space.

Fig. 6 shows a visualization via PCA of the 60 baseline data and the subsequent 200 observations. The results of the six features applied to the unprocessed signals (time domain), the vector of the wavelet coefficients (joint time-frequency domain), and the reconstructed signals (time domain) are shown in Figs. 6(a), 6(b), and 6(c), respectively. The propagation of the first anti-symmetric mode is considered. Ideally eleven distinct clusters should be observed: one cluster corresponding to the baseline and ten clusters corresponding to acquisitions 4 to 13. These ten clusters should be distinct as the acquisitions were made, according to Fig. 3(b), at distinct damaged conditions of the structure.

It is clear that the baseline (denoted by the filled diamonds) is well separated from the damaged data. Once more an uncertainty for the data 61-80 is revealed. The 2-dimensional visualization (PC1, PC2 plane) is affected by the domain used for the analysis. For instance, the joint time-frequency domain represented in Fig. 6(b) does not provide a clear clustering of the damaged data. The plots 6(a) and 6(c) show a quasi-linear path of the clusters as the size of the fatigue crack increases. In addition, the data associated with the reconstructed signals (Fig. 6(c)) get increasingly further away from the pristine condition enhancing the sensitivity of the method to small crack detection. The monotonic responses observed in Figs. 6(a) and 6(c) suggest that the damage index increases as the damage progresses. This behavior was observed in Fig. 5. However, the advantage

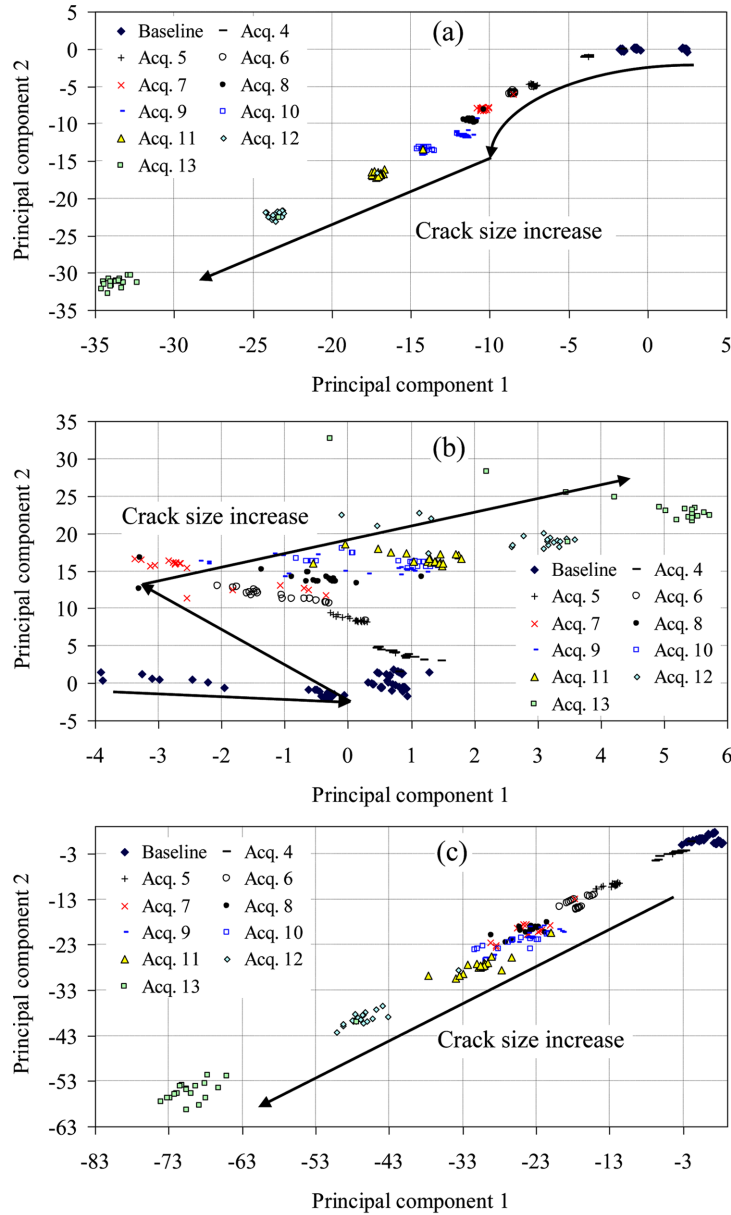


Fig. 6 Propagation of the first anti-symmetric mode : PCA visualization of the two principal components obtained from the analysis of the 6-dimensional damage index vector computed from the (a) original unprocessed waveforms, (b) wavelet coefficients vectors and (c) DWT-reconstructed waveforms

of the PCA with respect to the analysis of the single damage index component is evident in terms of damage sensitivity, i.e., the increase of damage indicators as the crack size progresses.

The lines superimposed in Fig. 6 show the path taken in the 2-dimensional space as the damage increases. The features in the time domain (Figs. 6(a) and 6(c)) show linear monotonicity and the data get increasingly further away as the fatigue cracks size increases. However, the path observed

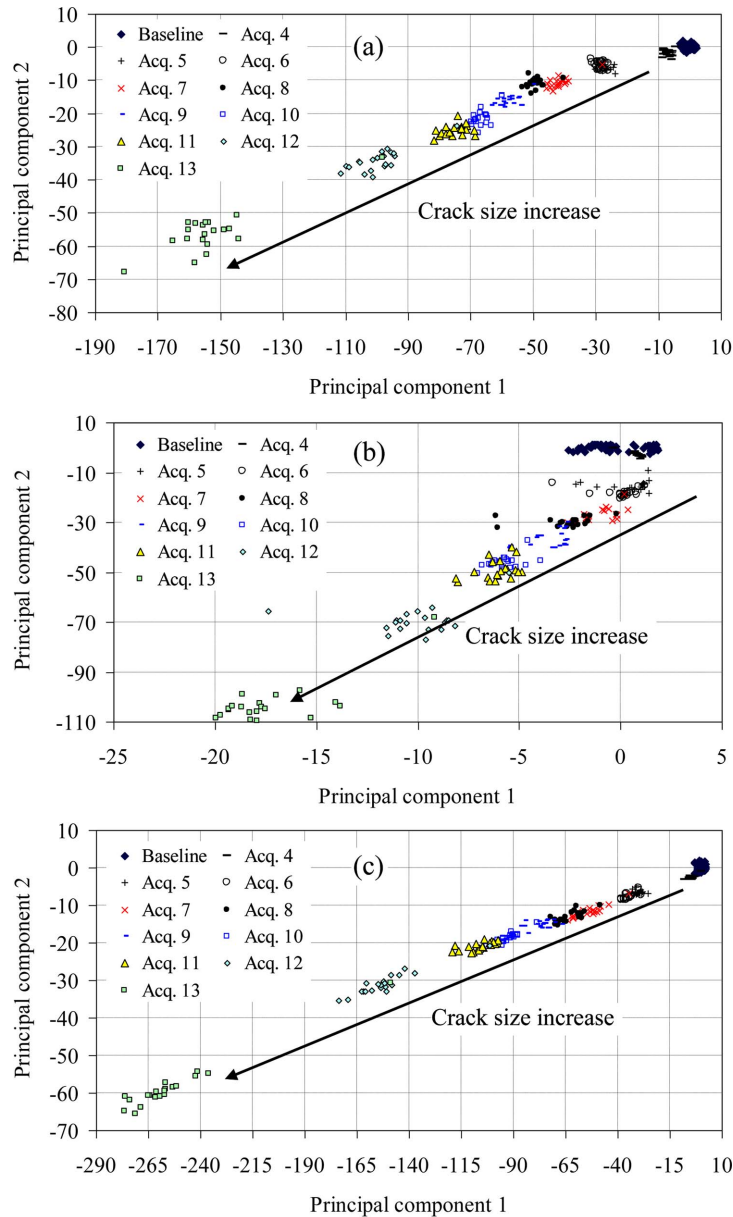


Fig. 7 Propagation of the first symmetric mode : PCA visualization of the two principal components obtained from the analysis of the 6-dimensional damage index vector computed from the (a) original unprocessed waveforms, (b) wavelet coefficients vectors and (c) DWT-reconstructed waveforms

from the analysis of the wavelet coefficient vector denotes a movable pattern.

A similar analysis was applied to the propagation of the first symmetric mode. The PCA visualization is presented in Fig. 7. Overall the plots show the same behavior found examining the A_0 mode. The values of both principal components are however, further away when compared to the equivalent data associated with the anti-symmetric mode. This means that the propagation of the S_0 mode is more effective than the propagation of the A_0 for detecting small crack size.

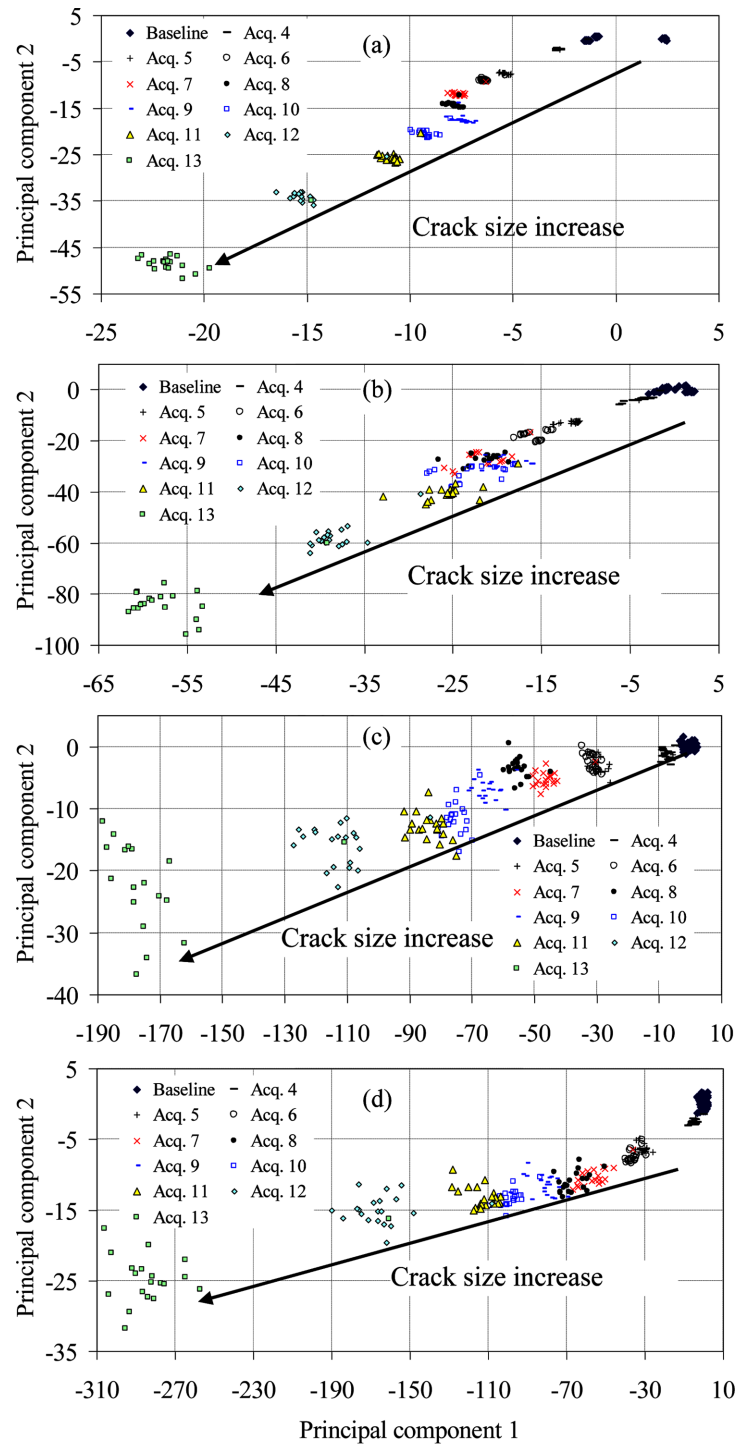


Fig. 8 PCA visualization of the two principal components obtained from the analysis of a 3-dimensional damage index vector computed from (a) original unprocessed A_0 waveforms, (b) DWT-reconstructed A_0 waveforms, (c) original unprocessed S_0 waveforms and (d) DWT-reconstructed S_0 waveforms

To investigate whether and how the selection of the statistical features affects the performance of the PCA, a subset of three features was retained. These features were the RMS, variance and K-factor. Figs. 8(a) and 8(b) show the results of the analysis conducted on the original time waveforms and the wavelet-based de-noised signals, respectively, associated with the propagation of the A_0 mode. Figs. 8(c) and 8(d) present the same analysis applied to the S_0 mode. Overall the linear path is confirmed. Qualitatively the selection of the statistical features affects the sensitivity of the algorithm to discriminate between small variations of the crack size.

To assess the sensitivity to crack a possible approach is to evaluate the R-squared value of the linear interpolation of the data plotted in the 2-dimensional plane, and the Euclidean distance between data associated with damage and baseline data. Closer the R-squared value is to 1 and higher is the value of the Euclidean distance, higher is the probability that different crack sizes can be distinguished. However, it is worth pointing out that some experimental evidence is in contrast with this approach. Figs. 6(a) and 8(a) show a larger number of clusters, i.e., better discrimination among crack sizes, with respect to Figs. 6(c) and 8(c), respectively, despite the Euclidean distance of each datum in the cluster is smaller.

5. Conclusions

This paper presents a crack detection technique for metallic waveguides using agile PZT transducers. The aim is to propose and validate a structural health monitoring scheme valid for waveguides subject to fatigue loading. Particularly, the study presented here focuses on the detection of the onset and propagation of fatigue crack induced on a steel structural beam. The technique is based on ultrasonic guided waves, discrete wavelet transform and principal component analysis. Ultrasonic waves were generated and detected by using PZT-wafers connected to a NI-PXI data acquisition system. A windowed 225 kHz toneburst was used as signal excitation. The time waveforms were processed with the discrete wavelet transform to generate a set of relevant damage sensitive features used to construct a multi-dimensional damage index vector. Finally, the dimensionality of this vector is reduced by using a principal component analysis algorithm.

Several conditions of the beam were monitored. It was demonstrated that the choice of the propagating wave mode and the application of the wavelet transform combined with the selection of appropriate statistical features might be effective to detect the initiation of fatigue cracks and to discriminate among various crack sizes. Experimental evidences suggest that the vector of the damage index obtained by computing the statistical features from the unprocessed time waveforms allows to discriminate among different crack sizes. However, by applying the discrete wavelet transform it was observed a larger distance between the data associated with damage and the baseline data. For both unprocessed and reconstructed signals a monotonic the first two principal components and the crack size was observed.

The structural health monitoring paradigm presented in this paper is applicable to many structural components having waveguide geometry such as plates, rods and pipes. Depending on the specific application, the ultrasonic configuration (whether pulse-echo or pitch-catch), the discrete wavelet transform decomposition levels, as well as the features considered in the computation of the damage index may change.

Future research may be warranted to study the effect of different mother wavelets on the algorithm performance.

Acknowledgments

The support of the University of Pittsburgh to Mr. Cammarata through startup funding available to the second author is acknowledged. The third and fourth authors acknowledge the support of the Korea Science and Engineering Foundation (M20703000015-07N0300-01510) and the Korea Research Foundation (D00462). The authors would like to thank Dr. Kent Harries and former graduate student Mr. Sandeep Degala for the help in the preparation of the experimental setup. The experimental work was conducted in the Watkins Haggart Structural Engineering Laboratory at the University of Pittsburgh.

References

- Alleyne, D.N. and Cawley, P. (1996), "The excitation of Lamb waves in pipes using dry-coupled piezoelectric transducers", *J. Nondestruct. Eval.*, **15**(1), 11-20.
- Chondros, T.G., Dimarogonas, A.D. and Yao, J. (1998), "A continuous cracked beam vibration theory", *J. Sound Vib.*, **215**(1), 17-34.
- Duntelman, G.H. (1989), *Principal Components Analysis*, Sage Publisher, Newbury Park, CA.
- Dutta, D., Sohn, H., Harries, K.A. and Rizzo, P. (2009), "A nonlinear acoustic technique for crack detection in metallic structures", *Struct. Health Monit.*, **8**(3), 251-262.
- Flury, B. (1988), *Common principal components and related multivariate models*, Wiley Publisher, New York, NY.
- Fromme, P. and Sayir, M.B. (2002), "Monitoring of fatigue crack growth at fastener holes using guided Lamb waves", *Proceedings of the AIP Conference, Review of progress in Quantitative Nondestructive Evaluation*, **615**, 247-254.
- Fromme, P., Lowe, M.J.S., Cawley, P. and Wilcox, P.D. (2004), "On the sensitivity of corrosion and fatigue damage detection using guided ultrasonic waves", *Proceedings of the IEEE Ultrasonic Symposium*, **2**, 1203-1206.
- Giurgiutiu, V. and Rogers, C.A. (1997), "Electro-mechanical (E/M) impedance method for structural health monitoring and non-destructive evaluation", *Proceedings of the International Workshop on Structural Health Monitoring*, 433-444.
- Giurgiutiu, V. (2005), "Tuned lamb wave excitation and detection with piezoelectric wafer active sensors for structural health monitoring", *J. Intel. Mat. Syst. Str.*, **16**(4), 291-305.
- Gupta, S., Ray, A. and Keller, E. (2007), "Symbolic time series analysis of ultrasonic data for early detection of fatigue damage", *Mech. Syst. Signal Pr.*, **21**(2), 866-884.
- Hotelling, K. (1933), "Analysis of a complex of statistical variables into principal component", *J. Educ. Psychol.*, **24**(6), 417-441.
- Jolliffe, I.T. (2002), *Principal component analysis* (2nd Edition), Springer, New York, NY.
- Johnson, M. (2002), "Waveform based clustering and classification of AE transients in composite laminates using principal component analysis", *NDT&E Int.*, **35**, 367-376.
- Kim, S.B. and Sohn, H. (2008), "Continuous fatigue crack monitoring without baseline data", *Fatigue Fract. Eng. Mater. Struct.*, **31**(8), 644-659.
- Kundu, T. (2004), *Ultrasonic Nondestructive Evaluation: Engineering and Biological Material Characterization*, CRC Press, USA.
- Leong, W.H., Staszewski, W.J., Lee, B.C. and Scarpa, F. (2005), "Structural health monitoring using scanning laser vibrometry: III. Lamb waves for fatigue crack detection", *Smart Mater. Struct.*, **14**, 1387-1395.
- Mallat, S.G. (1989), "A theory for multiresolution signal decomposition: the wavelet representation", *IEEE Trans. Pattern Anal. Mach. Intell.*, **11**, 674-693.
- Mallat, S.G. (1999), *A Wavelet Tour of Signal Processing*, Academic Press, New York, NY.
- Manson, G., Worden, K., Holford, K., Pullin, R. (2001), "Visualisation and dimension reduction of acoustic emission data for damage detection", *J. Intel. Mat. Syst. Str.*, **12**(8), 529-536.

- Mustapha, F., Manson, G., Pierce, S.G. and Worden, K. (2005), "Structural health monitoring of an annular component using a statistical approach", *Strain*, **41**(3), 117-127.
- Mustapha, F., Worden, K., Pierce, S.G. and Manson, G. (2007), "Damage detection using stress waves and multivariate statistics: an experimental case study of an aircraft component", *Strain*, **43**(1), 47-53.
- Ni, Y.Q., Zhou, X.T. and Ko, J.M. (2006), "Experimental investigation of seismic damage identification using PCA-compressed frequency response functions and neural networks", *J. Sound Vib.*, **290**(1-2), 242-263.
- Paget, C.A., Grondel, S., Levin, K. and Delebarre, C. (2003), "Damage assessment in composites by lamb waves and wavelet coefficients", *Smart Mater. Struct.*, **12**(3), 393-402.
- Park, G., Sohn, H., Farrar, C.R. and Inman, D.J. (2003), "Overview of piezoelectric impedance-based health monitoring and path forward", *Shock Vib. Dig.*, **35**(6), 451-463.
- Park, S., Yun, C.B. and Roh, Y. (2006), "Active sensing-based real-time nondestructive evaluations for steel bridge members", *KSCE J. Civil Eng.*, **10**(1), 33-39.
- Pearson, K. (1901), "On lines and planes of closest fit to systems of points in space", *Philos. Mag.*, **2**(6), 559-572.
- Rippengill, S., Worden, K., Holford, K.M. and Pullin, R. (2003), "Automatic classification of AE patterns", *Strain*, **39**, 31-41.
- Rizzo, P. and Lanza di Scalea, F. (2005), "Ultrasonic inspection of multi-wire steel strands with the aid of the wavelet transform", *Smart Mater. Struct.*, **14**(4), 685-695.
- Rizzo, P. and Lanza di Scalea, F. (2006), "Wavelet-based feature extraction for automatic defect classification in strands by ultrasonic structural monitoring", *Smart Struct. Syst.*, **2**(3), 253-274.
- Rizzo, P. and Lanza di Scalea, F. (2007), *Wavelet-based unsupervised and supervised learning algorithms for ultrasonic structural monitoring of waveguides*, *Progress in Smart Materials and Structures Research*, Ed. Peter L. Reece, NOVA Science Publishers, New York.
- Rizzo, P., Sorrivi, E., Lanza di Scalea, F. and Viola, E. (2007), "Wavelet-based outlier analysis for guided wave structural monitoring: application to multi-wire strands", *J. Sound Vib.*, **307**(1-2), 52-68.
- Rizzo, P., Cammarata, M., Dutta, D., Sohn, H. and Harries, K.A. (2009), "An unsupervised learning algorithm for fatigue crack detection in waveguides", *Smart Mater. Struct.*, **18**(2), 025016 (11pp), doi:10.1088/0964-1726/18/2/025016.
- Roberts, T.M. and Talebzadeh, M. (2003), "Acoustic emission monitoring of fatigue crack propagation", *J. Constr. Steel Res.*, **59**(6), 695-712.
- Rose, J.L. (1999), *Ultrasonic Waves in Solid Media*, Cambridge University Press, United Kingdom.
- Scala, C.M. and Bowles, S.J. (2000), "Laser ultrasonics for surface-crack depth measurement using transmitted near-field", *Proceedings of the AIP Conference, Review of progress in Quantitative Nondestructive Evaluation*, **509**, 327-334.
- Sharma, S. (1996), *Applied multivariate techniques*, John Wiley, New York, NY.
- Sohn, H., Worden, K. and Farrar, C.R. (2002), "Statistical damage classification under changing environmental and operational conditions", *J. Intel. Mat. Syst. Str.*, **13**(9), 561-574.
- Sophian, A., Tian, G.Y., Taylor, D. and Rudlin, J. (2001), "Electromagnetic and eddy current NDT: a review", *Insight*, **43**(5), 302-306.
- Staszewski, W.J. (2003), "Structural health monitoring using guided ultrasonic waves", *Proceedings of the AMAS & ECCOMAS Workshop/Thematic Conference SMART'03 on Smart Materials and Structures*, Jadwisin, Poland, September.
- Staszewski, W.J., Lee, B.C. and Traynor, R. (2007), "Fatigue crack detection in metallic structures with Lamb waves and 3D laser vibrometry", *Meas. Sci. Technol.*, **18**, 727-739.
- Tong, F., Tso, S.K., Hung, M.Y.Y. (2006), "Impact-acoustics-based health monitoring of tile-wall bonding integrity using principal component analysis", *J. Sound Vib.*, **294**(1-2), 329-340.
- Worden, K., Pierce, S.G., Manson, G., Philp, W.R., Staszewski, W.J. and Culshaw, B. (2000), "Detection of defects in composite plates using Lamb waves and novelty detection", *Int. J. Syst. Sci.*, **31**, 1397-1409.
- Yan, A.M., Kerschen, G., De Boe, P. and Golinval, J.C. (2005a), "Structural damage diagnosis under varying environmental conditions—Part I: A linear analysis", *Mech. Syst. Signal Pr.*, **19**(4), 847-864.
- Yan, A.M., Kerschen, G., De Boe, P. and Golinval, J.C. (2005b), "Structural damage diagnosis under varying environmental conditions—Part II: local PCA for non-linear cases", *Mech. Syst. Signal Pr.*, **19**(4), 865-880.